Analysis and evaluation of idler absorption for quasi-parametric chirped-pulse amplification

Dongxia Hu (胡东霞)[1,2], Yudong Tao (陶昱东)[2], Jingui Ma (马金贵)[3], Jing Wang (王 静)[3,*], Heyuan Zhu (朱鹤元)[1,], and Liejia Qian (钱列加)[3]**

[1]*Shanghai Engineering Research Center of Ultra-precision Optical Manufacturing, Department of Optical Science and Engineering, Fudan University, Shanghai 200433, China*

[2]*Research Center of Laser Fusion, China Academy of Engineering Physics, Mianyang 621900, China*

[3]*Key Laboratory for Laser Plasmas (Ministry of Education), Collaborative Innovation Center of IFSA (CICIFSA), Department of Physics and Astronomy, Shanghai Jiao Tong University, Shanghai 200240, China*

**Corresponding author: wangj1118@sjtu.edu.cn; **corresponding author: hyzhu@fudan.edu.cn*

Received August 16, 2018; accepted October 22, 2018; posted online November 28, 2018

Quasi-parametric chirped-pulse amplification (QPCPA) can improve the signal amplification efficiency and stability by inhibiting the back-conversion, in which the idler absorption plays a critical role. This Letter theoretically studies the impacts of idler absorption on the QPCPA performance in both the small-signal and saturation regimes. We demonstrate that there exists an optimal idler absorption that enables the achievement of maximum pump depletion within a minimum crystal length. To overcome the reduction in small-signal gain induced by idler absorption, the configuration of gradient idler absorption is proposed and demonstrated as a superior alternative to constant idler absorption. The results provide guidelines to the design of state-of-the-art QPCPA lasers.

OCIS codes: 190.4410, 190.4970.
doi: 10.3788/COL201816.121901.

Optical parametric chirped-pulse amplification (OPCPA) has been widely applied for generating ultrashort and ultra-intense lasers at devisable wavelengths[1,2]. Recently, quasi-parametric chirped-pulse amplification (QPCPA) is proposed as a promising alternative and has been demonstrated to be more efficient and more robust than OPCPA[3–5]. OPCPA is implemented with a nonlinear crystal transparent to all of the interacting waves, which is generally subject to the back-conversion effect that is detrimental to signal amplification efficiency and stability in the saturated regime. QPCPA, by introducing selective absorption at the idler wavelength, enables a unidirectional energy transfer from the pump to the signal, which can fully deplete the pump. As a result, QPCPA possesses the combined advantages of a high gain like OPCPA and a non-parametric saturation behavior like classical laser amplifiers. Besides, QPCPA allows efficient signal amplification regardless of a large phase mismatch, thus opening a gateway to build nonlinear amplifiers with unconventional media (e.g., semiconductor chips), where the perfect phase-matching condition is difficult to satisfy[6].

To push QPCPA for wider applications in state-of-the-art ultra-intense lasers, it is necessary to establish the design method to ensure the best performance. As a quite mature technique, the design of conventional OPCPA has been extensively studied, including the optimization of the broadband phase-matching configuration[7–9] and spatiotemporal shaping of the pump and signal[10–14]. These design considerations have contributed to the success of petawatt-level lasers[15], as well as intense few-cycle pulses[16,17] nowadays. As to QPCPA, the amplification behavior additionally depends on the configuration of idler absorption, which has not been addressed so far. A weak absorption might not sufficiently deplete the idler wave and thus cannot inhibit back-conversion, while a strong absorption will cause a considerable reduction in the small-signal gain. Either case would prolong the reaching of the ultimate efficient amplification; hence, high efficiency and stability are achieved by QPCPA at the expense of a longer crystal. In terms of ultrashort intense lasers, a longer crystal might cause the detrimental effects of dispersion, gain narrowing, and Kerr nonlinearity[18]. In this Letter, we focus on the optimization of idler absorption for the purpose of minimizing the QPCPA crystal length. Based on analytical derivations and numerical simulation, the impacts of idler absorption on both the small-signal gain and saturated conversion efficiency are quantified. Additionally, to overcome the gain reduction in current QPCPA systems with constant idler absorption, QPCPA with gradient absorption along the crystal is proposed and studied for the first time to the best of our knowledge.

Similar to conventional OPCPA, QPCPA is a three-wave-mixing process that can be described by coupled-wave equations, and all the three interacting waves are quasi-monochromatic at each temporal slice. Under the condition of group-velocity matching, the local approximation remains satisfied[19,20], and thus QPCPA can be temporally sliced into a group of independent narrowband amplifiers with their own instantaneous frequencies of the signal and idler. An integration of these narrowband calculations gives the performance of a broadband QPCPA. Consequently, the broadband coupled-wave equations can be reduced to the equations only in the

spatial domain, in which the dispersion effects are implicitly considered in the phase-mismatch term:

$$\frac{\partial A_i}{\partial z} = i\frac{\omega_i d_{\text{eff}}}{n_i c} A_p A_s^* e^{i\Delta k z} - \frac{\alpha_i(z)}{2} A_i, \tag{1a}$$

$$\frac{\partial A_s}{\partial z} = i\frac{\omega_s d_{\text{eff}}}{n_s c} A_p A_i^* e^{i\Delta k z}, \tag{1b}$$

$$\frac{\partial A_p}{\partial z} = i\frac{\omega_p d_{\text{eff}}}{n_p c} A_s A_i e^{-i\Delta k z}, \tag{1c}$$

where A_m ($m = p, s, i$) represents the complex amplitude of the pump, signal, and idler waves, respectively, with ω_m and n_m denoting their angular frequencies and refractive indexes. z is the propagation direction. d_{eff} is the effective nonlinear coefficient, and c is the speed of light in vacuum. $\Delta k = k_p - k_s - k_i$ with $k_m = n_m\omega_m/c$ refers to the phase mismatch between three waves. $\alpha_i(z)$ denotes the position-dependent absorption coefficient at the idler wavelength. Table 1 presents the parameters used in numerical calculations throughout this work. A spatiotemporal top-hat pump laser is first assumed, so it provides a uniform gain within the pulse duration and beam width. The seeding ratio $I_s(0)/I_p(0)$ is assumed to be 10^{-6} unless specified. We adopt the Sm^{3+}-doped yttrium calcium oxyborate (SmCOB) crystal for QPCPA, which exhibits a strong absorption in the spectral range of 1050 to 1600 nm[21]. This crystal absorbs the idler wave (at 1544 nm) in our simulated case, but does not absorb the pump (527 nm) and signal (800 nm). Except for the ion of Sm^{3+}, YCOB is also chemically compatible with other rare-earth ions, such as Tm^{3+} and Tb^{3+}, which have different absorption spectra and thus support QPCPAs at various signal wavelengths.

In the case of constant idler absorption [*i.e.*, $\alpha_i(z) \equiv \alpha$] and phase matching (*i.e.*, $\Delta k = 0$), the intensity growths of the signal and idler in the small-signal amplification regime have analytical solutions as

$$I_s(z) = I_s(0)\left[\cosh^2(gz) + \left(\frac{\alpha}{4g}\right)^2 \sinh^2(gz)\right]\exp\left(-\frac{\alpha}{2}z\right), \tag{2a}$$

Table 1. Default Simulation Parameters in This Letter

	Parameter	Value
Seed	Central wavelength	800 nm
	Bandwidth	30 nm
	Stretched pulse duration	1 ns
Pump	Wavelength	527 nm
	Duration	1 ns
	Intensity	4 GW/cm^2
SmCOB	Effective nonlinear coefficient	0.9 pm/V

$$I_i(z) = \frac{\omega_i}{\omega_s} I_s(0) \times \left(\frac{g_0}{g}\right)^2 \sinh^2(gz)\exp\left(-\frac{\alpha}{2}z\right), \tag{2b}$$

where I_s and I_i refer to the signal and idler intensities that are related to the complex amplitude A_s and A_i in Eq. (1) as $I_m = 1/2\varepsilon_0 c n_m |A_m|^2$, with the vacuum permittivity ε_0. The growth of the signal and idler is determined by the parametric gain coefficient g defined by

$$g = \sqrt{\frac{\alpha^2}{16} + \frac{2\omega_s\omega_i d_{\text{eff}}^2 I_p}{\varepsilon_0 n_s n_i n_p c^3}}. \tag{3}$$

Note that, with $\alpha = 0$ (*i.e.*, no idler absorption), this coefficient reduces to the small-signal gain coefficient of conventional OPCPA known as

$$g_0 = g(\alpha = 0) = \sqrt{\frac{2\omega_s\omega_i d_{\text{eff}}^2 I_p}{\varepsilon_0 n_s n_i n_p c^3}}. \tag{4}$$

In our case (Table 1), the crystal SmCOB provides a gain coefficient of $g_0 = 4\ \text{cm}^{-1}$ at the pump intensity of $I_p = 4\ \text{GW/cm}^2$. In practice, to obtain a reasonably high gain, we generally design a QPCPA with $\alpha \ll 4g_0$. Under this condition, Eqs. (2a) and (2b) can be further simplified to

$$I_s(z) = I_s(0)\cosh^2(g_0 z)\exp\left(-\frac{\alpha}{2}z\right), \tag{5a}$$

$$I_i(z) = \frac{\omega_i}{\omega_s} I_s(0)\sinh^2(g_0 z)\exp\left(-\frac{\alpha}{2}z\right). \tag{5b}$$

Compared to the solution of signal gain in OPCPA[19], it is apparent that an effective absorption with a coefficient of $\alpha/2$ is imposed onto the signal [Eq. (5a)] in QPCPA. Owing to this effective signal absorption, the dynamic absorption coefficient of the idler wave, during the nonlinear interaction, is accordingly reduced from α (without amplification) to $\alpha/2$ (with amplification), as indicated by Eq. (5b). Figure 1 illustrates the evolution of signal and idler intensities versus the crystal length (z), as well as the pump depletion ratio η_p that is defined as

$$\eta_p = 1 - \frac{\int I_p(z,t)\,\mathrm{d}t}{\int I_p(z=0,t)\,\mathrm{d}t}, \tag{6}$$

calculated for QPCPA with the idler-absorption coefficient $\alpha = 2\ \text{cm}^{-1}$ (the left column) and that with $\alpha = 5\ \text{cm}^{-1}$ (the right column), respectively. The results highlight that the above analytical solutions (dotted lines) match well with rigorous numerical solutions (solid lines) prior to significant pump depletion (*i.e.*, $\eta_p < 50\%$). This agreement provides confidence in the use of Eqs. (2) and (5) to estimate the small-signal gain of QPCPA.

Next, we characterize the impact of idler absorption on the saturation behavior of QPCPA based on numerical

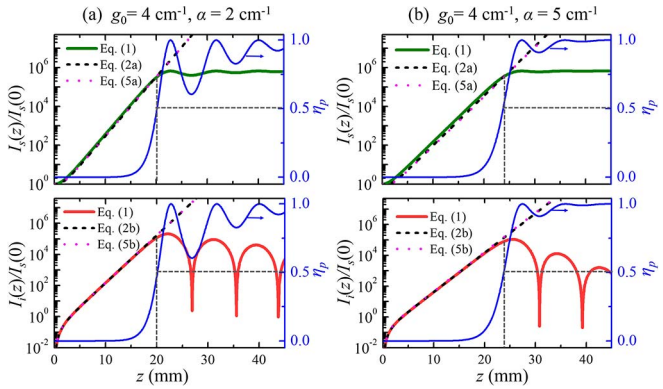

Fig. 1. Numerical solutions of signal gain $I_s(z)/I_s(0)$ (green solid lines) and idler intensity $I_i(z)/I_s(0)$ (red solid lines) and pump depletion ratio η_p (blue lines) versus crystal length z for QPCPA with (a) $\alpha = 2$ cm^{-1} and (b) $\alpha = 5$ cm^{-1}, respectively. The corresponding analytical solutions calculated with Eqs. (2) and (5) are plotted as dashed and dotted lines, respectively, for comparison.

calculations. Figure 2 gives the pump depletion versus crystal length calculated for QPCPA running with fixed pump intensity I_p and varied idler-absorption coefficient α. Here, the crystal length (x axis) is normalized to the characteristic length z_0, at which the OPCPA (*i.e.*, $\alpha = 0$) reaches its first maximum pump depletion ($z_0 = 20.21$ mm in our case). For conventional OPCPA, the pump depletion presents periodical oscillations between the parametric down-conversion and back-conversion, as shown in Fig. 2(a). However, such an

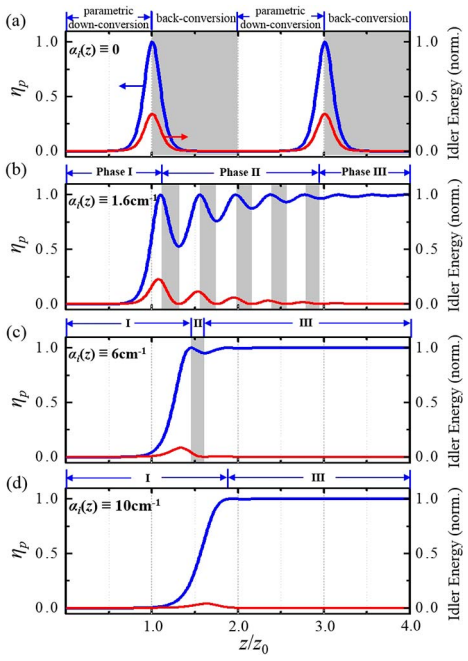

Fig. 2. Pump depletion curves (blue lines) for (a) OPCPA with $\alpha = 0$ and QPCPAs with (b) $\alpha = 1.6$ cm^{-1}, (c) $\alpha = 6$ cm^{-1} and (d) $\alpha = 10$ cm^{-1}, respectively. The red lines plot the evolution of idler energy (normalized to the initial pump energy).

oscillation behavior can be dramatically altered in the presence of idler absorption. For example, the conversion process in QPCPA with $\alpha = 1.6$ cm^{-1} can be classified into three phases. Initially, the parametric down-conversion dominates (termed as Phase I), wherein the signal increases monotonically. When reaching the maximum pump depletion, back-conversion occurs, and the process is then characterized by damped oscillations between down-conversion and back-conversion (termed as Phase II) due to idler absorption. During the damped oscillations, the oscillation period is gradually shortened, and the extent of back conversion shrinks until pump depletion approaches 100%. At the same time, the idler wave becomes fully dissipated by idler absorption, as depicted by the red line in Fig. 2(b). Since only the signal wave is left in the crystal, back-conversion will no longer occur, and the conversion process falls into the final phase (Phase III). To practically achieve high efficiency and stability, we generally design QPCPA in Phase III[3]. Apparently, Phase II is an undesired phase induced by the insufficient removal of the idler wave. It can be significantly shortened by adopting a stronger idler absorption. As in our case, Phase II is reduced to only one period of back-conversion by increasing α to 6 cm^{-1} [Fig. 2(c)]. Consequently, QPCPA falls into Phase III with a crystal length shortened by ~1/3 compared to that in QPCPA with $\alpha = 1.6$ cm^{-1} [Fig. 2(b)]. The strengthening of idler absorption, on the other hand, inevitably prolongs the length of Phase I due to the reduction of small-signal gain [Fig. 2(d)]. Therefore, an optimal α that enables the QPCPA to fall into Phase III with a minimum crystal length shall exist.

Let us first study the optimal absorption coefficient for QPCPA with constant idler absorption. Figures 3(a)–3(c) illustrate the contour of pump depletion against the crystal length (z/z_0) and idler-absorption coefficient (α/g_0) calculated for different parameter configurations. These contour maps highlight the existence of a critical value of α, termed α_c. For $\alpha < \alpha_c$, back conversion still occurs. While with $\alpha > \alpha_c$, the pump energy flows into the signal unidirectionally. It is obvious that only with the optimal absorption $\alpha = \alpha_c$, QPCPA can reach the ideal saturation of full pump depletion within a minimum crystal length. Despite the different QPCPA parameters in Figs. 3(a)–3(c), the ratio of the critical idler-absorption coefficient to the gain coefficient g_0 is found to be consistently approximated to

$$\frac{\alpha_c}{g_0} \approx \frac{4}{3}. \tag{7}$$

In Figs. 3(e)–3(f), we extend the comparison of α_c predicted by Eq. (7) (red circles) with the numerical result (blue circles) extracted from the pump depletion contour for a wider range of QPCPA parameters beyond those listed in Figs. 3(a)–3(c). These results illustrate that Eq. (7) generally holds true for QPCPA with weak

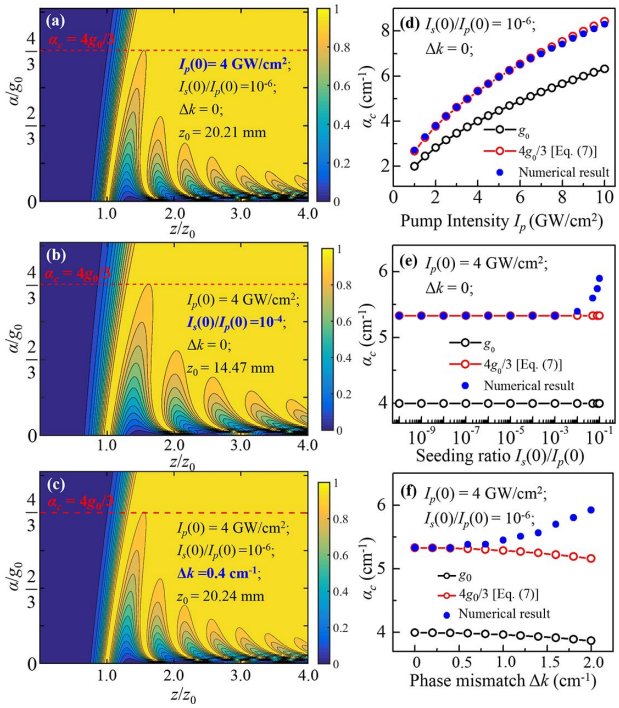

Fig. 3. (a), (b), (c) Contour maps of pump depletion η_p versus the crystal length z/z_0 and idler-absorption coefficient α/g_0 for QPCPAs pumped by a spatiotemporal top-hat pulse. The contour lines for η_p are plotted with a resolution of ~0.08. (d), (e), (f) The critical idler-absorption coefficients versus pump intensity I_p, seeding ratio $I_s(0)/I_p(0)$, and phase mismatch Δk, respectively. The blue solid circles and red open circles plot the results from numerical simulations and the empirical formula of Eq. (7), respectively.

seeding $[I_s(0)/I_p(0) \leq 10^{-2}]$ and small phase mismatch $(\Delta k < 0.1 g_0)$.

For an actual QPCPA system, the idler-absorption coefficient α is fixed, given a specific crystal, while the pump intensity (I_p) or the related gain coefficient (g_0) can be adjusted as a variable design parameter. According to Eq. (7), the optimal pump intensity can be deduced as

$$I_p\big|_{\text{opt}} = \frac{9\varepsilon_0 n_s n_i n_p c^3}{32\omega_s \omega_i d_{\text{eff}}^2} \times \alpha^2. \tag{8}$$

Such optimal pump intensity enables the suppression of back-conversion with a minimum crystal length. Nevertheless, in the QPCPA case with non-optimal pump intensity, the conversion efficiency will not be degraded considerably when the crystal is relatively long. As an example, Fig. 4(a) presents the pump depletion contour-map for QPCPA with $\alpha = 5.3$ cm^{-1}, which corresponds to the optimal idler absorption for pump intensity at 4 GW/cm^2. Apparently, although the pump intensity varies from 2 to 5 GW/cm^2, QPCPA maintains a unidirectional conversion that eventually approaches full pump depletion. By contrast, the pump depletion and signal conversion efficiency change with the pump intensity

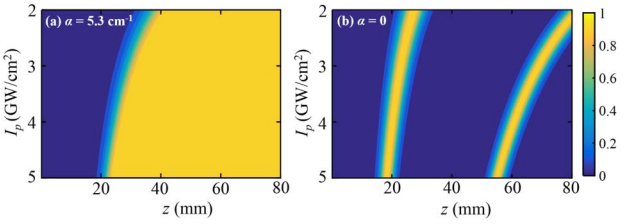

Fig. 4. Pump depletion contour map versus the crystal length z and initial pump intensity I_p for (a) QPCPA with $\alpha_i(z) = 5.3$ cm^{-1} and (b) OPCPA with $\alpha_i(z) = 0$, respectively.

dramatically in the case of conventional OPCPA, as indicated by Fig. 4(b).

In particular, if the pump has a spatiotemporal profile in a Gaussian shape rather than a top-hat one, the gain coefficient g_0 varies across the pulse duration and beam width. In this case, optimal α should be the weighted average of the critical idler-absorption coefficient at each spatiotemporal coordinate. Numerical simulations indicate [Fig. 5(a)] that the optimal α for a Gaussian-pumped QPCPA is $0.4g_0$, where g_0 refers to the peak gain coefficient governed by the peak pump intensity. By contrast, for the case of nonuniform absorption spectrum, Eq. (7) will still be valid if α_c is substituted with the averaged absorption coefficient. To illustrate this, Fig. 5(c) presents the efficiency curves for QPCPAs with uniform (blue line) and nonuniform (red line) absorption across the idler spectral range of 1490 to 1600 nm [Fig. 5(b)] in comparison. The results show a good agreement in terms of the crystal length required to achieve the non-parametric saturated amplification.

The configuration of a constant idler absorption inevitably induces a reduction of small-signal gain. To overcome this drawback, we propose and study the configuration of a gradient idler absorption along the crystal, in which the idler absorption is very weak in the initial amplification stage and gradually becomes strong in the saturated amplification regime. As an example, let us consider the QPCPA with a gradient idler absorption in form of a step function [Fig. 6(a)]:

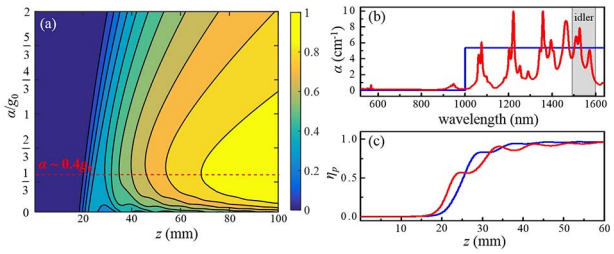

Fig. 5. (a) Contour map of the pump depletion ratio versus the crystal length z and idler-absorption coefficient α/g_0 calculated for QPCPA pumped by a spatiotemporal Gaussian pulse. For other parameters, see Table 1. (b) Two different idler-absorption spectra and (c) their corresponding efficiency curves. The pump is assumed to be spatiotemporally top-hat in (b) and (c).

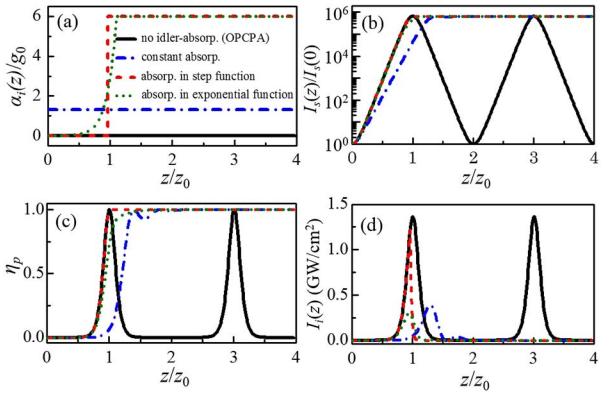

Fig. 6. Comparison of (a) idler-absorption coefficient, (b) signal gain, (c) pump depletion, and (d) idler intensity in OPCPA (solid lines) and QPCPAs with a constant absorption (dash dot lines), a step absorption function (dashed lines), and an exponential gradient absorption function (dotted lines), respectively.

$$\alpha_i(z) = \begin{cases} 0, & \text{when } z < 0.95z_0 \\ 6g_0, & \text{when } z \geq 0.95z_0 \end{cases}. \tag{9}$$

Since there is no idler absorption in the initial stage of amplification, the small-signal gain of this QPCPA is exactly equal to that in OPCPA [Fig. 6(b)]. Correspondingly, QPCPA under this case reaches its maximum pump depletion at a crystal length similar to that in OPCPA [Fig. 6(c)]. To suppress back-conversion, an idler absorption of $\alpha = 6g_0$ is introduced into the latter part of the crystal. Such a strong absorption depletes the idler wave quickly [Fig. 6(d)], thereby enabling stable QPCPA right at the first maximum pump depletion [Fig. 6(c)]. Such a QPCPA performance is most desired, because the idler absorption eliminates the back-conversion without any reduction in small-signal gain.

Besides the strict step function, QPCPA with other kinds of gradient idler absorption, such as an idler absorption that grows exponentially along the crystal, can achieve similarly favorable performance. The green dotted lines in Figs. 6(a)–6(d) characterize the QPCPA performance with a gradient idler-absorption function given by

$$\alpha_i(z) = \begin{cases} \exp(350z) - 1, & \text{when } z < 1.1z_0 \\ 6g_0, & \text{when } z \geq 1.1z_0 \end{cases}. \tag{10}$$

In this case, the reduction in small-signal gain is also negligible [Fig. 6(b)], while the back-conversion effect is completely suppressed. As indicated by Fig. 6(c), it is apparent that QPCPA with such a gradient idler-absorption configuration reaches the stable non-parametric saturation amplification much faster than the QPCPA with constant absorption.

In conclusion, we have demonstrated that in the presence of idler absorption, a QPCPA process can be divided into three amplification phases: initially a monotonic parametric down-conversion, intermediately damped oscillations between down-conversion and back-conversion, and finally a stable non-parametric saturation amplification with the full depletion of both pump and idler. The optimal idler absorption that eliminates the intermediate oscillations and lets the QPCPA reach the stable non-parametric saturation amplification with a minimum crystal length has been obtained based on numerical simulation and fitting. We further demonstrate that the reduction in small-signal gain by idler absorption in QPCPA systems nowadays can be well circumvented by adopting the configuration of gradient absorption. The results presented in this work can be readily applied to the design of state-of-the-art QPCPA-based ultraintense lasers.

This work was partially supported by the National Natural Science Foundation of China (NSFC) (Nos. 61727820 and 11721091) and the Science and Technology Commission of Shanghai Municipality (No. 17YF1409100).

References

1. Z. Xu and R. Li, Chin. Opt. Lett. **5**, S1 (2007).
2. M. Hemmer, A. Thai, M. Baudisch, H. Ishizuki, T. Taira, and J. Biegert, Chin. Opt. Lett. **11**, 013202 (2013).
3. J. Ma, J. Wang, P. Yuan, G. Xie, K. Xiong, Y. Tu, X. Tu, E. Shi, Y. Zheng, and L. Qian, Optica **2**, 1006 (2015).
4. J. Ma, J. Wang, P. Yuan, G. Xie, and L. Qian, Chin. Opt. Lett. **15**, 021901 (2017).
5. J. Ma, J. Wang, B. Zhou, P. Yuan, G. Xie, K. Xiong, Y. Zheng, H. Zhu, and L. Qian, Opt. Express **25**, 25149 (2017).
6. R. El-Ganainy, J. I. Dadap, and R. M. Osgood, Opt. Lett. **40**, 5086 (2015).
7. X. Guo, C. Wang, Y. Leng, and R. Li, J. Opt. Soc. Am. B **31**, 2615 (2014).
8. D. Herrmann, L. Veisz, R. Tautz, F. Tavella, K. Schmid, V. Pervak, and F. Krausz, Opt. Lett. **34**, 2459 (2009).
9. J. Bromage, C. Dorrer, and J. D. Zuegel, Opt. Lett. **35**, 2251 (2010).
10. I. N. Ross, P. Matousek, G. H. C. New, and K. Osvay, J. Opt. Soc. Am. B **19**, 2945 (2002).
11. J. Moses, C. Manzoni, S. Huang, G. Cerullo, and F. X. Kaertner, Opt. Express **17**, 5540 (2009).
12. J. Moses and S. Huang, J. Opt. Soc. Am. B **28**, 812 (2011).
13. L. J. Waxer, V. Bagnoud, I. A. Begishev, M. J. Guardalben, J. Puth, and J. D. Zuegel, Opt. Lett. **28**, 1245 (2003).
14. M. J. Guardalben, J. Keegan, L. J. Waxer, V. Bagnoud, I. A. Begishev, J. Puth, and J. D. Zuegel, Opt. Express **11**, 2511 (2003).
15. C. Danson, D. Hillier, N. Hopps, and D. Neely, High power Laser Sci. Eng. **3**, e3 (2015).
16. J. Rothhardt, S. Hädrich, J. C. Delagnes, E. Cormier, and J. Limpert, Laser Photon. Rev. **11**, 1700043 (2017).
17. S. Zhao, X. Zhou, P. Li, and Z. Chen, Phy. Rev. A **78**, 1830 (2008).
18. A. Thai, C. Skrobol, P. K. Bates, G. Arisholm, Z. Major, F. Krausz, S. Karsch, and J. Biegert, Opt. Lett. **35**, 3471 (2010).
19. E. J. Grace, C. L. Tsangaris, and G. H. C. New, Opt. Commun. **261**, 225 (2006).
20. S. Witte and K. S. E. Eikema, IEEE J. Sel. Top. Quantum Electron. **18**, 296 (2012).
21. Y. Tu, Y. Zheng, X. Tu, K. Xiong, and E. Shi, CrystEngComm **15**, 6244 (2013).